AN ADAPTIVE MONOPULSE PROCESSOR FOR ANGLE ESTIMATION IN A MAINBEAM JAMMING AND COHERENT INTERFERENCE SCENARIO

Yaron Seliktar [1,2] *E. Jeff Holder* [2] *Douglas B. Williams* [1]

[1]Center for Signal and Image Processing, School of ECE, Georgia Institute of Technology, Atlanta, GA USA
[2]Georgia Tech Research Institute, Georgia Institute of Technology, Atlanta, GA USA

ABSTRACT

Mainbeam jamming poses a particularly difficult challenge for conventional monopulse radars. In such cases spatially adaptive processing provides some interference suppression when the target and jammer are not exactly co-aligned, but the resulting array pattern is too distorted to be suitable for monopulse processing. The presence of coherent multipath in the form of terrain scattered interference (TSI) is normally considered a nuisance source of interference. However, it can also be exploited to suppress mainbeam jamming with space-time processing. Here we present a method for incorporating space-time processing into monopulse processing to yield a space-time monopulse processor with distortionless spatial array patterns that can achieve far better mainbeam jamming cancelation and target angle estimation than has been previously possible. Performance results for the monopulse processor are obtained for Mountaintop data containing a jammer and TSI, that demonstrate a dramatic improvement in performance over conventional monopulse and spatially adaptive monopulse.

1. INTRODUCTION

Tracking radars require a higher precision angular measurement of a target's azimuth (or elevation) than can be attained through standard processing techniques. The purpose of monopulse processing is to achieve the angular precision required for target tracking. Historically, monopulse radars employed two separate feed horns on a single antenna element in order to generate two receive beams that were slightly offset in azimuth (or elevation) angle. Sum and difference outputs were formed by summing and subtracting the two beam outputs, respectively. The ratio of difference to sum output voltages, called the error voltage, was then used to determine the degree of correction necessary to realign the beam axis with the target.

With the introduction of phased array technology it became unnecessary to employ special hardware for monopulse processing, since the array itself can electronically form the multiple beams needed. A typical conventional monopulse processor for a phased array radar is obtained by appropriately phasing the individual array channels to obtain sum and difference outputs. The ratio of difference to sum outputs provides the measure by which the angle offset from the beam axis (i.e., look direction) is determined. The updated angle measurement is then used to recompute phases for the channels so as to realign the beam axis with the target.

Mainbeam jamming occurs when the jammer signal is directly impinging on the radar's receive beam, obscuring targets that fall in its path. Spatially adaptive processing works well when target and jammer are adequately separated in angle. However, as the separation diminishes until target and jammer both appear within the mainbeam, performance degrades. This degradation is most severe when the target and jammer are co-aligned and the spatially adaptive processor is unable to achieve any cancelation at all. The problem of using a spatially adaptive processor is further compounded in that its pattern can become very distorted in the presence of mainbeam jamming.

In [1, 2] it is shown that the coherent multipath commonly referred to in the radar literature as *terrain scattered interference (TSI)* can be exploited to significantly improve interference mitigation performance. The operation of this processor is based on the principle that the direct path jammer can be used to predict and thus cancel the delayed jammer reflections from the ground (i.e., TSI) present in the mainbeam. Conversely, TSI can be used to estimate and cancel the direct path jammer in the mainbeam. The effectiveness of adaptive TSI processing for mitigating both TSI and mainbeam jamming motivates us to investigate ways of incorporating it with monopulse processing.

2. TSI PROCESSING

Considered here is a radar system that transmits a single pulse and samples the returns on an N element uniform linear array.[1] It collects L temporal samples from each element receiver, where each time sample corresponds to a *range cell*. The collection of samples is represented by an $N \times L$ data matrix $\mathbf{X}$ with elements $x(n,l)$. A *spatial snapshot* consists of N elements of spatial data from the t^{th} range cell (i.e., t^{th} column of $\mathbf{X}$)

$$\mathbf{x}(t) = \left[\begin{array}{cccc} x(0,l) & x(1,l) & \cdots & x(N-1,l) \end{array} \right]^T. \quad (1)$$

Similarly, a space-time snapshot, $\mathbf{X}(t)$, consists of T consecutive spatial snapshots in descending order (i.e., T consecutive descending columns of $\mathbf{X}$),

$$\mathbf{X}(t) = \left[\begin{array}{cccc} \mathbf{x}^T(t) & \mathbf{x}^T(t-1) & \cdots & \mathbf{x}^T(t-T+1) \end{array} \right]^T. \quad (2)$$

This work was partially supported by Wright Labs, USAF. Computing facilities used in this research are supported in part by the NSF under Grant MIP-9295853 and the Hewlett-Packard Company.

[1]In our notation, N denotes a scalar constant, $\mathbf{n}$ a spatial vector, and $\mathbf{N}$ a space-time vector or matrix.

The output, $z(t)$, is a weighted sum of the components of the space-time snapshot, $\mathbf{X}(t)$, at a given instant of time.

$$z(t) = \mathbf{W}^H \mathbf{X}(t). \tag{3}$$

Thus, the TSI processor is described by the $NT \times 1$ weight vector $\mathbf{W}$.

The simplest type of processing that can be performed on the data is nonadaptive spatial processing (i.e., where $T = 1$), also known as conventional processing. In conventional processing,

$$\mathbf{W} = \mathbf{v}(\nu_l) = \left[\begin{array}{cccc} 1 & e^{j2\pi\nu_l} & \cdots & e^{j2\pi\nu_l(N-1)} \end{array} \right]^T \tag{4}$$

is a spatial steering vector defined at spatial frequency $\nu_l = \frac{D}{\lambda}\sin(\phi_l)$, where ϕ_l is the target's look direction, D is the inter-element spacing of the array, and λ is the radar's operating wavelength [1].

Adaptive processing represents a more sophisticated class of processors and typically requires solving for a set of weights $\mathbf{W}$ that are optimal in the mean square sense. In other words, the mean square output of the processor,

$$\zeta = E\left\{|z(t)|^2\right\} = E\left\{\mathbf{W}^H\mathbf{X}\mathbf{X}^H\mathbf{W}\right\} = \mathbf{W}^H\mathbf{R}_\mathbf{X}\mathbf{W}, \tag{5}$$

is minimized with respect to $\mathbf{W}$ subject to the constraints $\mathbf{C}\mathbf{W} = \mathbf{c}$. The solution can be expressed in closed form as

$$\mathbf{W} = \mathbf{R}_\mathbf{X}^{-1}\mathbf{C}^H\left(\mathbf{C}\mathbf{R}_\mathbf{X}^{-1}\mathbf{C}^H\right)^{-1}\mathbf{c}. \tag{6}$$

The constraints are typically selected so as to satisfy two sets of conditions at the look direction ν_l: namely, unity gain at the first tap and zero gain at successive taps. The latter set of constraints are known as *range constraints* or *null constraints*. The constraint quantities are given as,

$$\mathbf{C} = \mathbf{I}_T \otimes \mathbf{v}^H(\nu_l) \qquad \mathbf{c} = \left[\begin{array}{cccc} 1 & 0 & \cdots & 0 \end{array} \right]^T, \tag{7}$$

where $\otimes$ denotes a Kronecker product. The resulting set of weights have the desirable property that a target at the look direction passes through the processor undistorted.

3. MONOPULSE PROCESSING

As mentioned earlier, a phased array monopulse processor requires both sum and difference output channels. In a nonadaptive configuration the sum processor is simply the steering vector, $\mathbf{W}_s = \mathbf{v}(\nu_l)$, as defined in (4). The difference processor is derived from the steering vector by phase reversing the latter half of its components.

$$\mathbf{W}_d = \mathbf{t}_d \odot \mathbf{v}(\nu_l), \tag{8}$$

where $\mathbf{t}_d = \left[\begin{array}{cc} \mathbf{1}_{1\times\frac{N}{2}} & -\mathbf{1}_{1\times\frac{N}{2}} \end{array} \right]^T$, [2] and $\odot$ denotes an elementwise matrix product. The effect of the phase reversal can be observed in Fig. 1, where a null at the look direction splits the mainlobe in two. The sum and difference outputs are given in terms of the respective processors,

$$z_s(t) = \mathbf{W}_s^H\mathbf{X}(t), \qquad z_d(t) = \mathbf{W}_d^H\mathbf{X}(t). \tag{9}$$

[2] A bold numeral denotes a vector or matrix all of whose elements are that value (i.e., $\mathbf{1}_{2\times3}$ is a 2×3 matrix of ones).

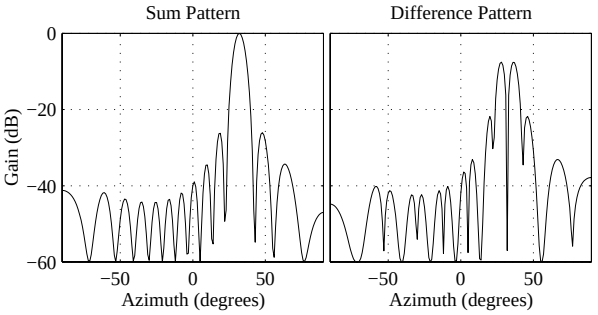

Figure 1: Two-Way Patterns for Sum and Difference Conventional Processor (Look Direction = 32°)

The imaginary part of the ratio of difference to sum outputs is known as the error voltage,

$$\epsilon_v(t) = \Im\left\{\frac{z_d(t)}{z_s(t)}\right\} \tag{10}$$

In general the ratio $\frac{z_d}{z_s}$ is imaginary-valued for a single target return and complex-valued for interference. The real part of the ratio is discarded since it is unrelated to the desired target. Once an error voltage is available, it can be used in conjunction with a *monopulse response curve (MRC)* to arrive at an angle estimate, $\hat{\phi}$, of the target's true azimuth ϕ.

The MRC, which plays a key role in monopulse processing, represents the ideal response of the monopulse processor (i.e., error voltage ϵ_v) to targets within the mainbeam. The spatial response of a space-time weight vector $\mathbf{W}$ is defined by $\mathcal{W}(\phi) = \mathbf{W}^H(T_0)\mathbf{v}(\phi)$, where $\mathbf{W}(T_0)$ denotes an $N \times 1$ vector comprised of the N weights in $\mathbf{W}$ corresponding to tap T_0. The MRC is defined as the imaginary part of the ratio of difference to sum responses.

$$\mathcal{M}(\phi) = \Im\left\{\frac{\mathcal{W}_d(\phi)}{\mathcal{W}_s(\phi)}\right\} \tag{11}$$

Figure 2 illustrates the response of a conventional monopulse processor to targets ranging in azimuth from 26° to 38.5°. Given an error voltage measurement, the target azimuth is determined by inverse mapping the error voltage through the MRC, $\hat{\phi} = \mathcal{M}^{-1}(\epsilon_v)$, as illustrated in Fig. 2.

In practice the processor pair $\mathbf{W}_s$ and $\mathbf{W}_d$ are not able to completely reject interference. The residual interference that is present in the imaginary component of $\frac{z_d}{z_s}$ causes the error voltage ϵ_v to deviate from its ideal value as given by the MRC. The corresponding error in the azimuth angle measurement, $\epsilon_\phi = \hat{\phi} - \phi$, is illustrated by the dashed lines in Fig. 2. One particularly useful performance measure for the monopulse processor is the *Standard Deviation of the Angle Error (STDAE)*

$$\sigma_{\epsilon_\phi} = \sqrt{\mathrm{E}\left\{|\epsilon_\phi|^2\right\}}. \tag{12}$$

Qualitatively, the flatter the MRC, the greater the resulting error in azimuth reading for a given deviation of error voltage. Therefore, it is desirable to have a "well sloped" curve such as the one shown in Fig. 2. Another desirable property of the conventional processor's MRC is that it be unbiased; that is, the curve passes through the coordinate $(\phi_l, 0)$.

We would like to develop a monopulse processor that

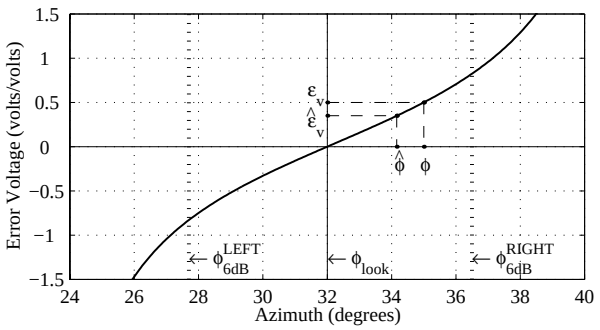

Figure 2: Conventional Monopulse Response Curve

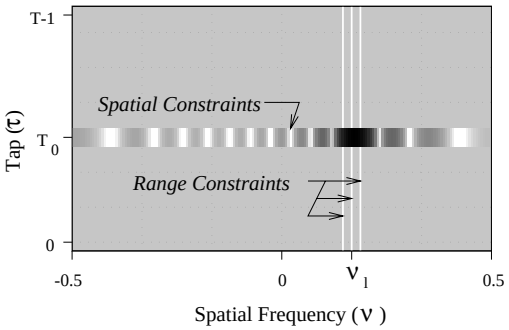

Figure 3: Constraint Specifications for the Space-Time Adaptive Monopulse Processor

has the desirable target response characteristics shown in Fig. 2 and, yet, provides adequate suppression of main beam jamming with minimal target spreading. The space-time processor considered is that of (6) with a set of constraints chosen to achieve these criteria.

Of the T taps in the processor, the T_0^{th} tap captures the target as shown in Fig. 3. In order to prevent target spreading in the look direction, range constraints are applied at the look direction (ν_l) for all taps except T_0 (shown as center white line in Fig. 3). Since the detected target may have been detected anywhere within the mainbeam, it is necessary to provide additional range constraints about the look direction at spatial frequencies, $\nu_l \pm 0.5/N$ (shown as additional white lines in Fig. 3). The additional range constraints do not ensure zero gain throughout the angular extent of the mainbeam but rather serve as "anchors" to keep the gain low in that region. The specified range constraints are implemented via a constraint matrix and vector,

$$\mathbf{C}_0 = \begin{bmatrix} \mathbf{I}_{T_0-1} & \mathbf{0}_{T_0-1\times T-T_0+1} \\ \mathbf{0}_{T-T_0\times T_0} & \mathbf{I}_{T-T_0} \end{bmatrix} \otimes \begin{bmatrix} \mathbf{v}^H(\nu_l - \frac{1}{2N}) \\ \mathbf{v}^H(\nu_l) \\ \mathbf{v}^H(\nu_l + \frac{1}{2N}) \end{bmatrix} \tag{13}$$

$$\mathbf{c}_0 = \mathbf{0}_{T-1\times 1} \tag{14}$$

Spatial response constraints (SRC) are defined for an expected target at tap T_0. Typically, a unity gain constraint (7) is used, but in the case of monopulse processing a more rigid set of constraints is necessary to ensure a reliable and robust MRC. This requirement is met most stringently by forcing the processor to take the form of a conventional processor at tap T_0, in which case the spatial response of the processor is identical to the one shown in Fig. 1. This condition can be met by applying the constraint matrix and vector,

$$\mathbf{C}_1 = \begin{bmatrix} \mathbf{0}_{1\times T_0} & 1 & \mathbf{0}_{1\times T-T_0-1} \end{bmatrix} \otimes \mathbf{I_N}, \tag{15}$$

$$\mathbf{c}_1 = \begin{cases} \mathbf{v}(\nu_l), & \text{if sum processor,} \\ \mathbf{t}_d \odot \mathbf{v}(\nu_l), & \text{if difference processor.} \end{cases} \tag{16}$$

An alternative and simpler method for implementing the SRC is to apply a large degree of diagonal loading to the portion of the covariance matrix $\mathbf{R_X}$ corresponding to T_0, and applying a unity gain constraint (i.e., $[\mathbf{I}_T(T_0) \otimes \mathbf{c}_1^H]\mathbf{W} = 1$, where $\mathbf{I}_T(T_0)$ is the T_0^{th} row of the identity matrix).

Grouping the range constraints with the spatial response constraints, we have the constraint matrix and vector

$$\mathbf{C} = \begin{bmatrix} \mathbf{C}_0 \\ \mathbf{C}_1 \end{bmatrix}, \qquad \mathbf{c} = \begin{bmatrix} \mathbf{c}_0 \\ \mathbf{c}_1 \end{bmatrix}. \tag{17}$$

The sum and difference processors are specified in terms of the design parameter T_0. The significance of T_0 is in the type of prediction that the resulting processor performs. In the example of Sec. 2 and in the derivations of [1, 2], a forward prediction filter is implemented by specifying that the target appear in the first tap (i.e., $T_0 = 0$). On the other hand, if the target is constrained to appear in the final tap (i.e., $T_0 = T - 1$), we have a backward prediction filter. As will be seen in Sec. 4, selecting a tap-centered configuration (i.e., $T_0 = T/2$) that corresponds to a combination of forward and backward prediction, yields the best monopulse performance for Mountaintop (MT) data.

4. SIMULATION RESULTS

Performance results for monopulse processing are obtained for MT dataset `mmit004v1` containing a direct path jammer at 32° and stationary TSI. The interference to noise ratio (INR) is 62 dB. The four processors considered are a conventional processor, a spatially adaptive processor with unity gain constraint, and two tap-centered space-time adaptive processors as described in Sec. 3: one with 20 taps and the other with 50.

Figure 4 shows the two-way sum pattern[3] for the 50 tap processor. The SRC appear at $T_0 = 25$ while the null constraints appear at $\phi_l = 32°$ and its vicinity. The artificially induced spatial response at T_0 imposes a sharp boundary between T_0 and adjacent taps. Methods of "relaxing" the SRC to achieve a more esthetic boundary have been considered; however, their application does not seem to significantly affect performance.

Performance results for mainbeam jamming are shown in Fig. 5. The space-time adaptive processors require less SNR to achieve a given value of STDAE. For instance, given a desired STDAE of 0.5°, the spatially adaptive processor requires 52 dB of SNR, whereas the 50 tap space-time processor requires only 37 dB of SNR – an improvement of 15 dB!

It is also interesting to see how the different processors fare in a non-mainbeam jamming scenario. In Fig. 6 we fix the SNR at 50 dB and vary the look azimuth from −70° to 70°. The resulting plot of STDAE performance versus

[3] A two-way pattern includes the pattern from a directional transmitter as opposed to the omni-directional transmitter assumed by a one-way pattern.

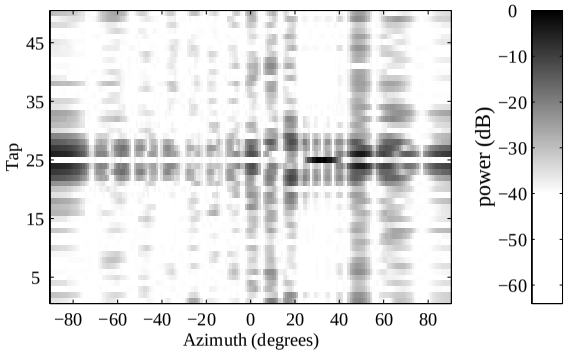

Figure 4: Two-Way Sum Pattern (`mmit004v1.mat`)

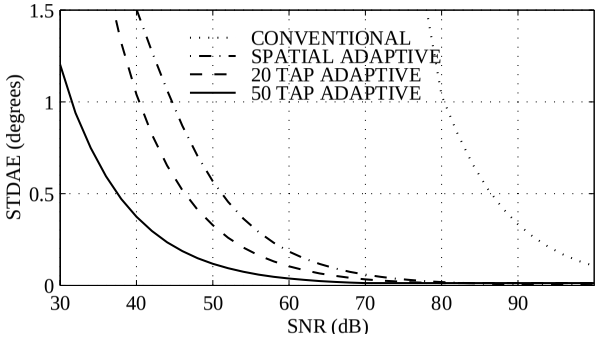

Figure 5: STDAE vs. SNR (Look Direction = 32°)

look azimuth is shown in Fig. 6 for the adaptive processors. The benefit of space-time over spatially adaptive monopulse processing in the case of non-mainbeam jamming is clear. We find that space-time processing performance can be improved even further in the non-mainbeam jamming case by applying fewer constraints and selecting different tap placement configurations. However, such variations do not prove robust in a mainbeam jammer scenario since the full set of constraints are necessary to prevent the sum and difference pattern distortions.

Similar test results for other datasets containing TSI are tabulated in Table 1. The 6 dB beamwidth (ϕ_{bw}) and output interference to noise ratio (OINR) for the sum processor are provided as additional performance measures. Typically OINR is the figure of merit for a TSI processor. However, as can be inferred from the results for the spatially adaptive processor, consistent OINR performance does not necessarily ensure consistent STDAE performance. The space-time processor does demonstrate consistent results for all datasets except for `mmit013v1` where the location of the jammer, namely at $\phi_l = 66.2°$, results in reduced angular resolution and, hence, a loss of STDAE performance.

5. CONCLUSIONS

The main innovation introduced in this paper is a method by which a monopulse processor is combined with an adaptive space-time processor to provide a precise angle tracking capability in the presence of TSI and mainbeam jamming. Key features of the new processor are a tap-centered configuration, extended range constraints, and spatial response constraints. Range constraints play a key role when the transmitted waveform is spread in time (e.g., linear FM)

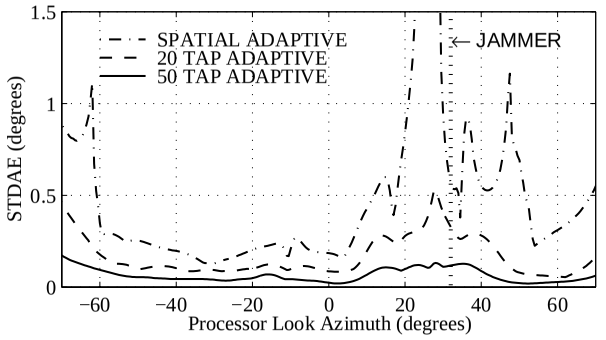

Figure 6: STDAE vs. Look Direction (Target SNR= 50dB)

	1 Tap Processor			50 Tap Processor		
Name	ϕ_{bw}	OINR	σ_{ϵ_ϕ}	ϕ_{bw}	OINR	σ_{ϵ_ϕ}
`mmit004v1`	5.85	31.0	0.57	8.80	21.5	0.12
`mmit013v1`	12.3	33.2	1.96	15.5	22.4	0.21
`mmit043v1`	5.65	25.1	0.19	8.80	21.8	0.13
`mmit044v1`	5.90	25.7	0.19	8.80	22.0	0.14
`mmit045v1`	5.95	23.3	0.16	8.80	19.4	0.09
`mmit048v1`	5.75	25.1	0.18	8.80	22.2	0.14
`mmit109v1`[a]	5.70	25.1	0.44	8.80	20.6	0.11
`mmit112v1`[a]	5.70	25.0	0.44	8.80	20.6	0.11

Table 1: Performance results for other MT datasets (SNR = 50 dB). See URL `www.mhpcc.edu` for more information on MT datasets.
[a]Contain TSI without a direct path jammer.

and pulse compression follows TSI processing. Range constraints in the look direction are intended to prevent spreading throughout the mainbeam, but the application of spatial constraints at T_0 imposes such a burden on the processor that spreading within the mainbeam becomes a problem. Therefore, additional range constraints about the look direction become necessary.

Previous work has shown no clear advantage to using different tap distributions. Here, however, for monopulse it has been demonstrated that a combination of forward and backward prediction is essential. We have verified that forward or backward prediction alone does not yield a viable processor when spatial response constraints are applied. However, without the spatial response constraints the processor performs inconsistently and is susceptible to distortions in the sum and difference responses; particularly, in a mainbeam jamming scenario.

6. REFERENCES

[1] S. M. Kogon, D. B. Williams, E. J. Holder, "Beamspace Techniques for Hot Clutter Cancelation", *ICASSP 96*, vol. 2, pp. 1177-1180, May 1996.

[2] S. M. Kogon, *Adaptive Array Processing Techniques for Terrain Scattered Interference Mitigation*, Ph.D. Thesis, Georgia Institute of Technology, 1997.

[3] S. M. Kogon, E. J. Holder, D. B. Williams, "On the Use of Terrain Scattered Interference for Mainbeam Jammer Suppression," *ASAP 97*, March 1997.

[4] S. M. Sherman, *Monopulse Principles and Techniques*, Artech House, Dedham, MA 02026, 1984.